Structural and vibrational analysis of nanocrystalline Ga 1 x Mn x N films deposited by reactive magnetron sputtering

J. H. Dias da Silva, D. M. G. Leite, A. Tabata, and A. A. Cavalheiro

Citation: Journal of Applied Physics **102**, 063526 (2007); doi: 10.1063/1.2783844
View online: http://dx.doi.org/10.1063/1.2783844
View Table of Contents: http://scitation.aip.org/content/aip/journal/jap/102/6?ver=pdfcov
Published by the AIP Publishing

Structural and vibrational analysis of nanocrystalline $Ga_{1-x}Mn_xN$ films deposited by reactive magnetron sputtering

J. H. Dias da Silva,[a] D. M. G. Leite, and A. Tabata
Depto. de Física, Advanced Materials Group, São Paulo State University-UNESP, Bauru SP 17033-360, Brazil

A. A. Cavalheiro
Depto. de Biociências, Advanced Materials Group, São Paulo State University-UNESP, Botucatu SP 18618–000, Brazil

(Received 21 June 2007; accepted 26 July 2007; published online 27 September 2007)

The structural and vibrational properties of nanocrystalline $Ga_{1-x}Mn_xN$ films deposited by reactive magnetron sputtering were analyzed in a wide composition range ($0<x<0.18$). The films were structurally characterized using x-ray diffraction with Rietveld refinement. The corresponding vibrational properties were investigated using micro-Raman and Fourier transform infrared spectroscopies. The films present a high crystallized fraction, crystallites having wurtzite structure, and high orientation texture with the *c* axis oriented perpendicular to the substrate surface. Rietveld analysis indicates that Mn atoms are incorporated substitutionally into Ga positions and show that the ionic character of cation-*N* bonds along the *c* axis is favored by the Mn incorporation. No evidence for Mn segregation or Mn rich phases was found in the composition range analyzed. Micro-Raman scattering spectra and infrared absorption experiments showed progressive changes with the increase of *x* and monotonic shifts of the GaN TO and LO peaks to lower frequencies. The structural and vibrational analyses are compared and the influence of Mn on the static and dynamic properties of the lattice is analyzed. © *2007 American Institute of Physics*.
[DOI: 10.1063/1.2783844]

I. INTRODUCTION

The diluted magnetic semiconductor $Ga_{1-x}Mn_xN$ is a promising candidate for spintronics applications.[1,2] The Curie temperature above 300 K and the increasing interest and control of the ferromagnetism are among the advantages of focusing on the properties of this material. The success of the preparation of ferromagnetic $Ga_{1-x}Mn_xN$ using the molecular beam epitaxy (MBE) technique is quite recent[3–7] and has attracted the attention of several groups concerning the mentioned as well as other techniques.[8–14]

In a recent report we have described the preparation of $Ga_{1-x}Mn_xN$ nanocrystalline films using the sputtering technique.[15] The low substrate temperature, allowed by the plasma breaking of N_2 molecules and the use a metallic Ga target covered by small Mn pieces, makes the preparation and Mn incorporation simple and versatile. Even though films prepared by sputtering are generally amorphous or polycrystalline, the recent improvement of the sputtering technique allowed the preparation of crystalline single domain GaN films,[16] indicating that crystalline $Ga_{1-x}Mn_xN$ can possibly be produced by this technique. Among the advantages of the sputtering technique is the possibility to grow the films at relatively low temperatures, resulting in more control on the phase separation during growth. The role of phase separation and its relation with the ferromagnetic properties in this material are at present under debate,[9,17,18] giving importance to the understanding of the Mn role while affecting the structural, vibrational, and electronic properties of the material.

The combination of x-ray diffraction and Raman scattering techniques has proved to reveal some of the most important structural and vibrational characteristics of the nanocrystalline materials.[7,9,10,19,20] In particular, the Rietveld refinement of the diffractograms can address thoroughly the question of phase formation and Raman scattering is efficient to reveal the presence of ordered polarization-dependent vibrational modes as well as structural disorder and local vibrational modes. Although the use of these techniques concerning the presence of nonmagnetic impurities in crystalline GaN is relatively well explored in the literature, the investigation related to the presence of magnetic elements presents only a few reports.[7,10]

In the present study the Rietveld refinement of x-ray diffraction, micro-Raman scattering, as well as Fourier transform infrared (FTIR) spectroscopy were applied to investigate the structural and vibrational properties of nanocrystalline $Ga_{1-x}Mn_xN$ films, which are produced by reactive sputtering in a wide Mn concentration range.

II. EXPERIMENTAL DETAILS

The films were prepared using the reactive rf magnetron sputtering technique. Pure (6*N*) N_2 atmosphere and a (7*N*) Ga target were utilized. The Mn was introduced into the films by covering the target with small Mn pieces. The Mn content in the compound was easily controlled using this technique. Samples were prepared on amorphous silica

[a]Author to whom correspondence should be addressed. Tel.: +55 (14) 3103-6178. FAX: +55 (14) 3103-6084. Electronic mail: jhdsilva@fc.unesp.br

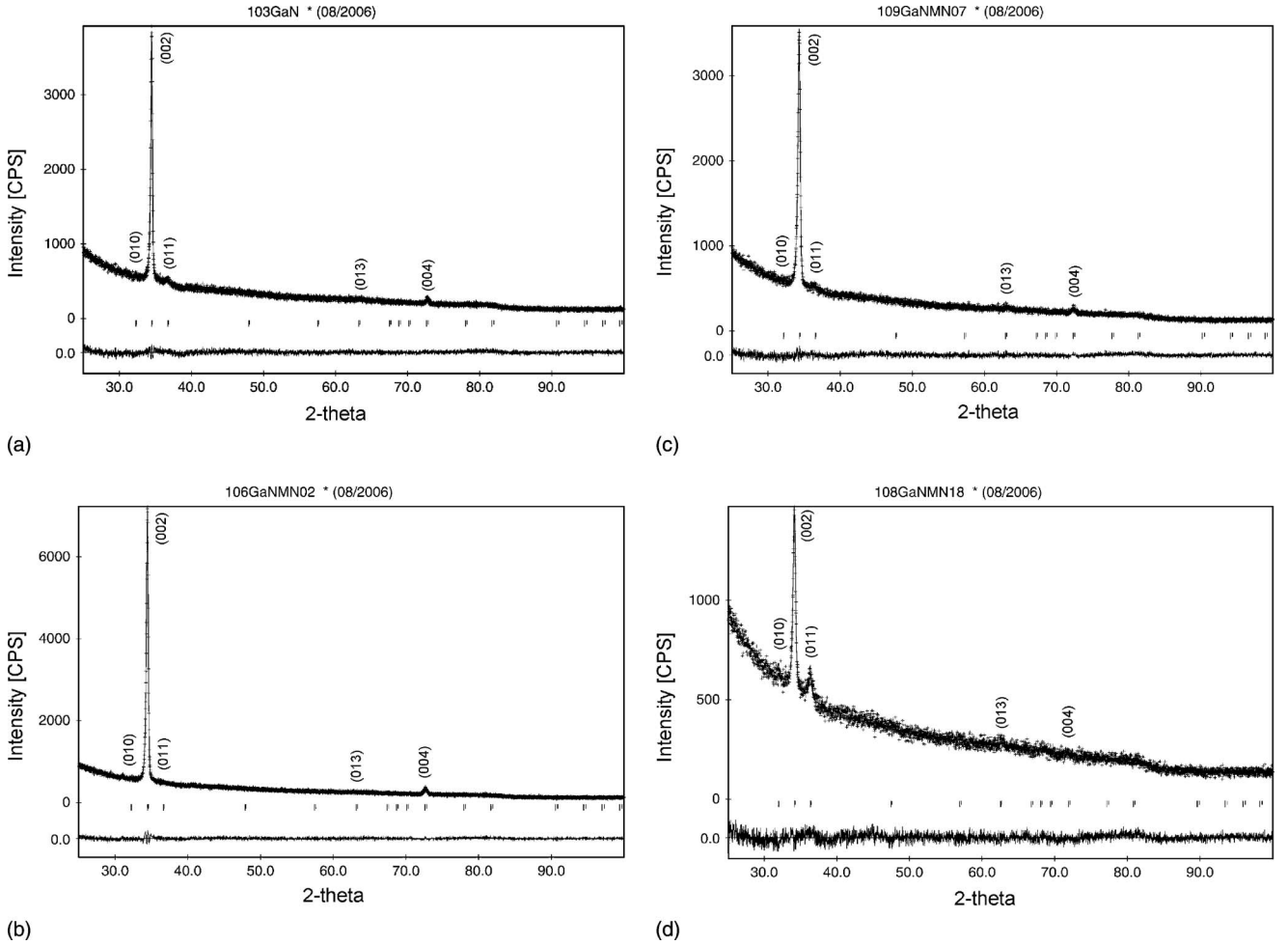

FIG. 1. Rietveld graphics for different compositions of $Ga_{1-x}Mn_xN$ films [(a)–(d)] deposited by reactive sputtering. Each figure [(a)–(d)] shows the observed pattern (dot line), calculated pattern (solid line), and the goodness of the fit or residual pattern (at the bottom), obtained from the difference between calculated and observed patterns. The corresponding refinement results are presented in Table I.

(a-SiO_2), Si (100), and GaAs(100) substrates. The collisions of the plasma energetic ions with the surface of the depositing films were minimized due to the use of a planar magnetron configuration with a relatively large (5 cm) target to substrate distance. More details about film preparation were given elsewhere.[15]

Oxygen contamination was not detected (neither in Raman nor in infrared—assigned to bands around 1000 cm^{-1}). Some H contamination was detected in association with bands present in 1590 cm^{-1} (assigned to Ga–H oscillations) and in 3500 cm^{-1} (assigned to N–H vibrations). Residual H_2 is also detected in the gas analysis prior to deposition, but not in the N_2 gas used. This was attributed to target contamination from the previously prepared GaN:H samples.[21]

The Ga/Mn ratio was measured by energy dispersive x-ray (EDX) spectroscopy, in a Zeiss DSM 960 scanning microscope. The Mn content was found to be directly proportional to the area covered by Mn in the target.[15] No direct measurement of the nitrogen content was made. Nevertheless, the similarity of the optical properties of the undoped films with crystalline GaN indicates that the composition is close to stoichiometry.[15,21]

X-ray diffraction experiments were performed in a θ-2θ geometry, using Cu $K\alpha$ radiation in a rotating anode setup (Rigaku-Ultima 2000+), with a K_β filter. A refinement of the measurements using the Rietveld method was performed with the Rietveld refinement program DBWS-9807.[22] The samples used in the analysis were the ones deposited onto amorphous silica. Tests on samples deposited on Si and GaAs oriented crystals did not show significant differences.

The micro-Raman scattering experiments were performed at room temperature using a Jobin-Yvon T64000 triple spectrometer in backscattering geometry. The Ar^+ 488.0 nm laser line was used as excitation. No light polarization analysis was used to carry out the experiments. Infrared absorption bands were measured in a Magna 760 FTIR spectrophotometer in samples deposited on Si and GaAs substrates.

III. RESULTS AND DISCUSSION

The deposition of nanocrystalline $Ga_{1-x}Mn_xN$ films by the reactive magnetron sputtering technique using a Ga target in N_2 atmosphere and Mn cosputtering was versatile and efficient. Films with compositions between $x=0.00$ and $x=0.18$ were produced using this technique[15]. The x-ray diffraction (XRD) patterns [Figs. 1(a)–1(d)] show that the structure of the films belongs to the $P63mc$ space group with

TABLE I. Refined structural data for $Ga_{1-x}Mn_xN$ films with different Mn contents obtained through the Rietveld refinement. Structure: hexagonal $P63mc$ (C_{6v}^4), $Z=2$, (Ref. ICSD: 25-676), Atomic positions: Ga^{+3} (1/3,2/3;0), Mn^{+3} (1/3,2/3;0), N^{-3} (1/3,2/3;z), where R_{Wp} is the refinement quality parameter, R_{Bragg} is the structural conformity parameter, and $\beta 11$ is the anisotropic displacement parameter. Lattice and bond parameters are also displayed, as well as the preferential orientation and density.

						Lattice parameters			(Ga)–N bond length (Å)			
Sample	x	R_{Wp}	R_{Bragg}	N^{-3} z coordinate	$^{\dagger}Ga^{+3}$ $\beta 11$	a (Å)	c (Å)	V (Å^3)	a and b directions	c direction	Prefer. orient. (%)	Density (g cm^{-3})
SP103	0.00	6.74	11.83	0.398	0.09	3.2039	5.2041	46.264	1.9245	2.0712	66	6.01
SP106	0.02	6.91	5.29	0.395	0.61	3.2070	5.2042	46.355	1.9303	2.0557	68	5.98
SP105	0.05	6.83	4.70	0.395	0.53	3.2111	5.2137	46.577	1.9329	2.0594	68	5.92
SP109	0.07	6.62	9.84	0.397	0.12	3.2161	5.2242	46.756	1.9330	2.0740	67	5.88
SP107	0.08	6.62	12.82	0.404	0.13	3.2219	5.2220	46.944	1.9264	2.1097	62	5.84
SP108	0.18	6.33	21.96	0.446	0.02	3.2316	5.2489	47.442	1.8873	2.3410	46	5.68

strong preferential orientation at the [002] direction. Using the Scherer formula and the diffraction peak width, we could estimate crystallite mean sizes of the order of 25 nm in all samples.

The data obtained by Rietveld refinement are shown in Table I. The preferential orientation parameter in the [002] direction, associated with the c axis perpendicular to the substrate surface, was calculated using the March-Dollase function. The data show that the samples with lower manganese concentrations (up to $x<0.07$) display higher degree of orientation, reaching approximately 68% in sample SP106. For higher Mn concentrations ($x>0.08$, Table I) the orientation degree decreases, indicating that higher amounts of manganese tend to break the long range ordering in c direction.

The lattice expansion caused by the manganese insertion, noticed by the increase of the unit cell volume from 46.264 (GaN) to 47.442 Å^3 ($x=0.18$), can be associated with the bigger size of the manganese as compared to gallium. This fact, associated with the smaller atomic weight of Mn (54.94 g mol^{-1}) compared with that of Ga (69.72 g mol^{-1}), causes also the decrease in the material density from 6.01 (GaN) to 5.68 g cm^{-3} ($x=0.18$). The increase in the unit cell volume as a consequence of the Mn insertion occurs almost isotropically with the a and c parameters increasing simultaneously. As a matter of fact, the ionic (covalent) radii of Ga^{+3}, Mn^{+3}, and N^{-3} in angstroms are 0.47 (0.61), 0.58 (0.72), and 1.46 (1.32), respectively,[23] thus the expected ionic and covalent Ga–N bond lengths for this structure are both 1.93 Å. It is interesting to notice that in spite of the monotonic increase in the lattice parameters ($a=b$ and c), the bond distances displayed in Table I exhibit a slightly different behavior. In a and b directions, the bond distance suffers firstly a slight increase (for small x) and later tends to decrease with the increase in the Mn content, being of the order of the sum of the covalent radii. On the other hand, the bond in c direction that is of order of the sum of the ionic radii presents a slight decrease with the first Mn incorporation and then increases continuously with the Mn content. The bond polarities and lengths that take place in this structure should play an important role in defining the preferential orientation texture observed in the films.

The nitrogen position ($N^{-3}z$ coordinate, Table I) remains practically unaffected until $x=0.07$, showing that the structure expands isotropically to receive low concentrations of the Mn cation in the Ga site. When the Mn concentration is further increased from this value, the nitrogen atoms leave their original positions, affecting also the rigid positions of the gallium site. This effect can be observed by the increasing in the R_{Bragg} factor, which is associated with correlation between the real structure with the proposed model. In spite of this, a good refinement quality was obtained for all of the samples, noticed by the R_{wp} factor, which presents values between 6% and 7%.

The thermal anisotropic parameter for the Ga sites ($\beta 11$) should be interpreted in association with the variations of the nitrogen coordinate ($N^{-3}z$) and the lattice parameters. The biggest oscillation of this parameter, corresponding to the oscillations of the Ga and Mn ions in the referred direction for the $x=0.02$ and $x=0.05$, can be understood as a consequence of the insertion of Mn in the lattice, since in these samples, the lattice expansion is not followed by the displacement of the N atom. As a consequence the cation sites are expanded raising the diffraction probability of these sites. With the increase of the Mn concentration above $x=0.05$ the nitrogen atoms are displaced toward $z=0.5$, demonstrating that the higher amounts of manganese require more space. This structural rearrangement comprises the gallium site in the ab plane, noticed by the decrease in the $\beta 11$ values. On the other hand, an increase in c is verified, causing the increase in Ga–N bond length. This event leads to the enhancement ionic character of the bond in the c direction, which is followed by the decrease of the preferential orientation of the crystallites.

The vibrational properties of the films were focused with the help of Figs. 2 and 3, which display the micro-Raman and infrared absorption results, respectively. Figure 2 shows the first order Raman scattering bands for films with different Mn contents. The peak positions corresponding to the transverse and longitudinal optical modes in the GaN bulk crystals are indicated by vertical lines. The dotted line in 578.5 cm^{-1} represents the vibrational frequency of a localized mode associated with the Mn,[7,8,24] which will be discussed ahead. A band associated with the acoustic modes of disordered GaN is also observed in 300 cm^{-1}.[10,12,19]

As it was expected for nanocrystalline films, the Raman spectra of the undoped material ($x=0$) presents intermediate

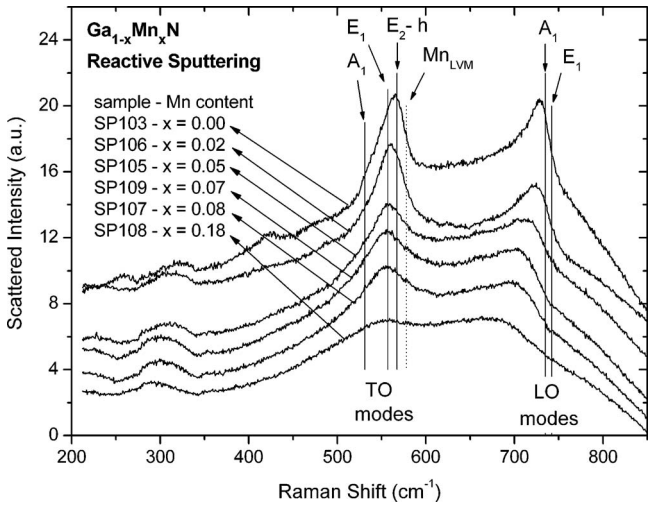

FIG. 2. Micro-Raman scattering spectra of $Ga_{1-x}Mn_xN$ films with different Mn concentrations, measured at room temperature using the Ar^+ 488.0 nm laser line excitation. The spectra were vertically shifted for clarity. The vertical solid lines indicate the positions of zone-center phonons in wurtzite GaN crystals (Ref. 19) and the vertical dotted line is located at the calculated Mn related impurity mode frequency (Ref. 8).

characteristics between the GaN crystal[19] and the spectrum of the corresponding amorphous[20] material. The bands associated with the sets of convoluted TO and LO modes are clear in the undoped sample, being the signal measured in the backscattering configuration without polarization. The observed bands are considerably broader and the component modes are not resolved, as compared to the observed in the GaN and $Ga_{1-x}Mn_xN$ bulk crystals: the reported LO-A_1 (TO-$E_{2\text{-high}}$) peak width is ~6 cm^{-1} (Ref. 25) [12 cm^{-1} (Ref. 19)], while in our samples the width of the LO (TO) band is approximately 32 cm^{-1} (30 cm^{-1}). In amorphous GaN with similar excitation (458 nm), the optical modes show up in a single band, with approximate width of 160 cm^{-1}, in which it is not possible to deconvolute the TO and LO bands.[20] In the amorphous case only a slight structure is observed in the broad optical band, and a clear raise in the scattering is observed at frequencies below 350 cm^{-1} in association with the acoustic modes.[20]

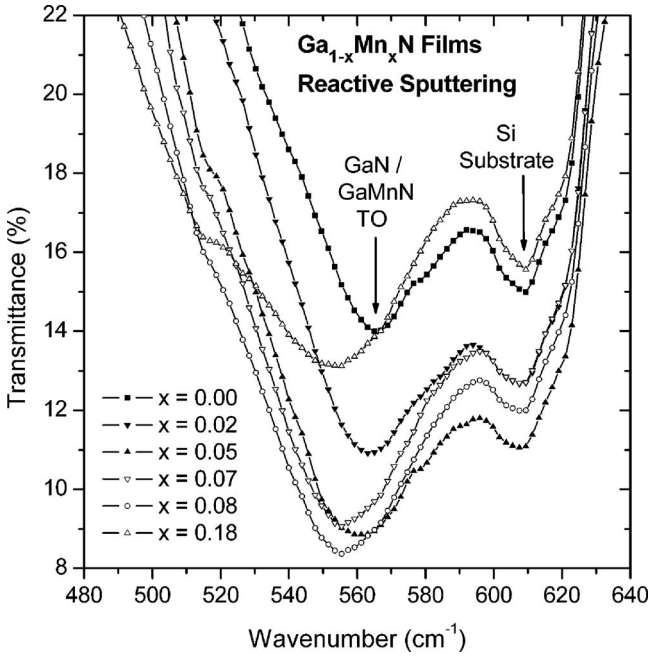

FIG. 3. Fourier transform infrared spectra in the spectral range corresponding to the band related to the TO modes of GaN/GaMnN films. The positions of the peaks are displayed in Fig. 4. Different curves correspond to different Mn contents. Bands related to the substrate absorption can also be noted in 512 and 610 nm, corresponding, respectively, to lattice vibration and impurity absorption of the Si wafer.

The broadening of the optical vibrational peaks in our spectra can be explained by the partial relaxing of the selection rules during scattering caused by the disorder of the lattice. In this way the scattering spectra also present the contribution of modes with wave vectors located outside the Brillouin zone center. Consistently, the shape of the spectrum of the nanocrystalline undoped sample resembles a broadened version of the vibrational mode density of states of the corresponding crystal[26] and with the density of states (DOS) extracted from neutron diffraction experiments.[27]

The influence of Mn in the vibrational properties of the $Ga_{1-x}Mn_xN$ films was noticed through general aspects of the changes produced in the spectrum, but no apparent specific band was found. The presence of Mn affects more intensively the band related to the LO modes due the anisotropic changes in the lattice parameters of the GaN structure caused by Mn insertion in the Ga site, which is consistent with the strong increase in the $\beta 11$ parameter for small x values (Table I). Effectively, with the increase of the Mn concentration, the shift of the LO peak to smaller frequencies, the weakening of its maximum intensity, and its broadening are observed. Reported polarized measurements[7] indicate that the disorder component associated with the presence of Mn in this peak is strong even in monocrystalline films produced by MBE.[7]

In a similar trend to the band related to the LO modes, the band associated with the TO modes displays a considerable broadening (full width at half maximum of ~30 cm^{-1}) when compared with measurements of particular vibrational modes reported for GaN crystals.[7,19] Also, if one considers the frequency superposition between this band and the crystal TO modes (Fig. 2), it can be concluded that the observed band corresponds to an overlapping of the E_1, E_2, and A_1 modes. The A_1 is not allowed in the crystal when the excitation is in the c-axis direction, but it can be present here by the effect of the disorder.

One component associated with a localized vibration mode (LVM) of Mn is expected at high frequency vicinity of the TO-E_2 peak.[7,8,24] The frequency of this mode, valid in the limit of low Mn concentration, can be estimated using the effective mass approximation,[7,8,24]

$$\omega_{\text{Mn-LVM}} = \omega_{\text{GaN}}^{\text{TO}} \sqrt{\frac{\mu_{\text{GaN}}}{\mu_{\text{MnN}}}}. \quad (1)$$

The estimation of this frequency for bulk $Ga_{1-x}Mn_xN$ (Ref. 8) and for films prepared by MBE (Ref. 7) gives the values of 574 and 586 cm^{-1}, respectively, while the same approximation in our samples results in 578 cm^{-1} (Table II). The broadening of the TO peak includes this frequency, even in the sample without Mn. In this way it is difficult to indi-

TABLE II. Wave numbers of values of the Raman bands maxima and FTIR minima for $Ga_{1-x}Mn_xN$ samples with different Mn contents.

Sample	x	Raman TO $\omega(cm^{-1})$	Raman LO $\omega(cm^{-1})$	FTIR TO $\omega(cm^{-1})$
SP103	0.00	565.9	728.0	565.7
SP106	0.02	560.4	723.9	563.2
SP105	0.05	558.1	715.0	560.7
SP109	0.07	557.6	704.1	555.5
SP107	0.08	556.3	698.1	554.6
SP108	0.18	556.5	674.6	554.3

vidualize a band at this frequency in our spectra, even though the changes in the line shape with the increasing Mn content are consistent with the existence of such band. In this way we did not succeed in individualizing a component associated with the localized Mn modes. Harima[7] observed that the detection with crossed polarization relative to the excitation in $Ga_{1-x}Mn_xN$ crystals promoted the individualization of a peak in 586 cm^{-1}, and consequently associated its presence with the TO-$E_{2\text{-high}}$ mode associated with the vibrations of Mn in Ga sites, which are known to present C_{3v} symmetry in the wurtzite lattice.

The TO-A_1 mode of the GaN–GaMnN is IR active, and Fig. 3 shows the absorption bands in FTIR spectra associated with this mode. The minimum of the transmittance spectrum (maximum of the absorption coefficient) tends to shift to lower frequencies to broaden and to increase the maximum absorption with the Mn content increase. The absorption increase and the shift observed are probably directly associated with the increase in polarity of the cation-N bonds in the c direction as function of Mn content, which was determined through the increase in the bond length values in c direction by the Rietveld method.

Either in IR absorption band maximum or in the Raman scattering peak, it is possible to notice that the frequency of the TO bands tends to be shifted to smaller frequencies with the increase of the Mn content, Fig. 4. Nevertheless, the amplitude of the shift is smaller in this case as compared with

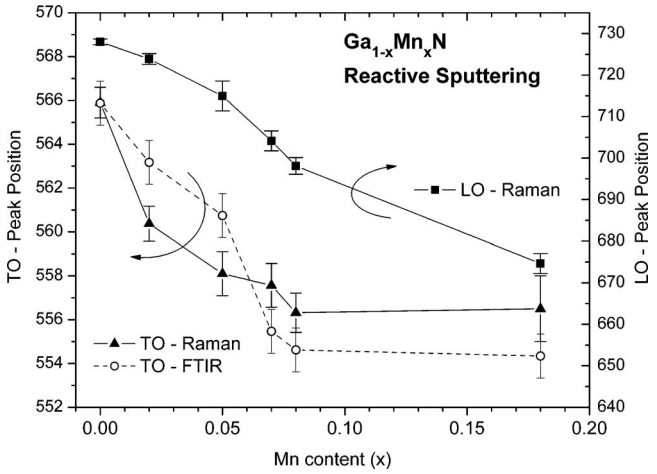

FIG. 4. Peak position related to the TO (left axis) and LO (right axis) vibration modes of $Ga_{1-x}Mn_xN$ compound, as determined by Raman and FTIR data (TO).

the observed shifting in the LO peak, as can be seen through the analysis of Fig. 4 and Table II. Concerning the TO mode, the shift occurs in the range limited by the TO-$E_{2\text{-high}}$ and TO-E_1 modes of the spectrum of the GaN crystal.

With the increase in the Mn content, the scattered intensities between the LO and TO peaks become increasingly important. The spectrum line shape presents well defined LO and TO bands when $x=0$, but evolves to a structure in which these peaks are almost completely convoluted when $x=0.18$. A similar behavior was reported for $Ga_{1-x}Mn_xN$ films with high Mn content and high disorder degree,[7,10] and can be understood, in general, as a result of disorder. In particular, the increases of both the N vacancies (dominant) and of the Mn_{LVM} peak component (minoritary) are expected to contribute to the scattering in the frequencies between the TO and LO peaks.

We could not notice in the spectra any characteristics directly related to the free carriers or to the interaction between carriers and vibrational modes. In n doped GaN the interaction with plasmons was reported to cause an important coupling with the LO modes, producing a shift of the corresponding peak to high frequencies,[19,28] while the p doping is expected to cause an increase in the scattering at low frequencies.[29]

The shift of the transmittance minima to smaller frequencies is represented in Fig. 4 together with the shifts of the Raman peaks. There is a close similarity between the shifts observed in the transmittance, related to the TO-A_1, mode and the Raman TO peak, which in our measurements is probably dominated by the $E2$-high modes. Based on known results for the Raman scattering in GaN (Ref. 19) and on the modifications in the line shape of the TO peak, we can speculate that for low Mn content and high orientation texture in the direction perpendicular to the substrate, the Raman TO band is dominated by the $E_{2\text{-high}}$ modes. Differently, when the Mn concentration is high and the orientation texture becomes weaker, it is probable that the Raman TO-A_1 and E_1, which have smaller frequencies, are raised, while the $E_{2\text{-high}}$ peak tends to decrease, since it is dependent on the alignment between the c axis and the incident beam normal to the substrate. Besides the decrease of the overall Raman scattering and the increase of the IR absorption are probably related to the increase of the polar character of the material bonds observed in the Rietveld analysis.

The disorder effect produced by the Mn insertion in Ga site is observed through the increase in the anisotropic displacement parameter for the Ga-site atoms ($\beta 11$), which is followed by a decrease in the film orientation texture. This result is consistent with the vibrational band broadening, redshifts, and the presence of acoustic bands. These lattice disorder effects can affect the magnetic properties of the material by changing carrier dynamics characteristics and consequently the interaction of carries with localized magnetic moments of the Mn ions with the lattice neighboring atoms.

Both the x-ray diffraction and the Raman scattering do not show any evidence of phase segregation, indicating that if there are segregated clusters, their occurrence is below the detection limit of these techniques. In the scanning electron

microscopy measurements we did not find composition differences in film surfaces with different superficial morphologies. The homogeneity of the samples is also evidenced in the micro-Raman spectra taken in different positions and in the regularity of the transmittance spectra in the visible and near infrared ranges.[15] Thus, we can conclude that in the films prepared by reactive sputtering under the conditions used, the cluster formation or phase segregation is absent or very small, that is, the produced material is essentially homogenous. In this way the $Ga_{1-x}Mn_xN$ nanocrystalline films produced by reactive sputtering are potential candidates to present interesting properties, such as ferromagnetism at temperatures above 300 K, in spite of the observed disorder effects. The magnetic characterization of the material will be addressed in a future work.

IV. CONCLUSIONS

The structural and vibrational properties of nanocrystalline $Ga_{1-x}Mn_xN$ films prepared by reactive cosputtering were analyzed in a wide composition range. A strong orientation texture in which the *c* axis of the wurtzite crystallites oriented perpendicular to the substrate surface is present in the material. With the progressive Mn incorporation, an increase in the bond length and in the ionic character of the cation-N bond along the *c* axis are observed. Correspondingly, the vibrational frequencies of the bands associated with the set of TO and LO modes decrease with the increase of the Mn content, indicating a weakening of the cation-N bond and an increase of the lattice disorder.

Through the structural refinement and spectroscopic techniques, it was shown that the vibrational changes originated from the Mn insertion in Ga site occur in a progressive way, while the structural changes do not. However, the combination of the results provide a clear mechanism to understand the modification in the structure of this material. The results indicate that the films do not display phase segregation and that the Mn substitutionally occupies the Ga sites in wurtzite crystallites. The obtained results are consistent with single phase nanocrystalline material.

ACKNOWLEDGMENTS

We would like to acknowledge the FAPESP agency (Grant Nos. 2005/02249-0, 2004/12120-1, and 2006/05627-8) for the financing, Professor Margarida Juri Saeki for the use of the FTIR equipment, and L. F. da Silva for the assistance with the x-ray diffraction measurements.

[1] T. Dietl, H. Ohno, F. Matsukura, J. Cibert, and D. Ferrand, Science **287**, 1019 (2000).
[2] S. J. Pearton *et al.*, J. Appl. Phys. **93**, 1 (2003).
[3] S. Kuwabara, T. Kondo, T. Chikyow, R. Ahmet, and H. Munekata, Jpn. J. Appl. Phys., Part 2 **40**, L724 (2001).
[4] M. E. Overberg, C. R. Abernathy, S. J. Pearton, N. A. Theodoropoulou, K. T. McCarthy, and A. F. Hebard, Appl. Phys. Lett. **79**, 1312 (2001).
[5] G. Thaler, R. Frazier, B. Gila, C. R. Albernathy, S. J. Pearton, and C. Segre, Appl. Phys. Lett. **84**, 1314 (2004).
[6] S. Sonoda, S. Shimizu, T. Sasaki, Y. Yamamoto, and H. Hori, J. Cryst. Growth **37–239**, 1358 (2002).
[7] H. Harima, J. Phys.: Condens. Matter **14**, R967 (2002).
[8] W. Gebiki, J. Strzeszewski, G. Kamler, T. Szyszko, and S. Podsiadlo, Appl. Phys. Lett. **76**, 3870 (2000).
[9] M. Zajac *et al.*, Appl. Phys. Lett. **78**, 1276 (2001).
[10] Y. Y. Yu *et al.*, J. Cryst. Growth **269**, 270 (2004).
[11] L. L. Guo, H. Zhang, and W. Z. Shen, Appl. Phys. Lett. **89**, 161920 (2006).
[12] Y. H. Zhang, L. L. Guo, and W. Z. Shen, Mater. Sci. Eng., B **130**, 269 (2006).
[13] S. Granville *et al.*, J. Appl. Phys. **100**, 084310 (2006).
[14] Y. K. Byeun, K. S. Han, H. J. Choi, and S. C. Choi, Mater. Sci. Eng., A, **452–453**, 499 (2007).
[15] D. M. G. Leite, L. F. da Silva, A. L. J. Pereira, and J. H. Dias da Silva, J. Cryst. Growth **294**, 309 (2006).
[16] Q. X. Guo, A. Okada, H. Kidera, T. Tanaka, M. Nishio, and H. Ogawa, J. Cryst. Growth **237**, 1079 (2002).
[17] M. Marques, L. K. Teles, L. M. R. Scolfaro, J. Furthmüller, F. Bechstedt, and L. G. Ferreira, Appl. Phys. Lett. **86**, 164105 (2005).
[18] I. T. Yoon, T. W. Kanga, and D. J. Kimb, Mater. Sci. Eng., B **134**, 49 (2006).
[19] N. E. Christensen and P. Perlin, in *Semiconductors and Semimetals*, edited by R. K. Willardson and E. R. Weber (Academic, New York, 1998), Vol. 50, Chap. 13, pp. 409–427.
[20] H. J. Trodahl, F. Budde, B. J. Ruck, S. Granville, A. Koo, and A. Bittar, J. Appl. Phys. **97**, 084309 (2005).
[21] D. M. G. Leite, A. L. J. Pereira, L. F. da Silva, and J. H. Dias da Silva, Braz. J. Phys. **36**, 978 (2006).
[22] R. A. Young, A. C. Larson, and C. O. Paiva-Santos, *User's Guide to Program DBWS-9807 for Rietveld Analysis* (Georgia Institute of Technology, Atlanta, 1998).
[23] R. D. Shannon, Acta Crystallogr., Sect. A: Cryst. Phys., Diffr., Theor. Gen. Crystallogr. **32**, 751 (1976).
[24] A. Kaschner *et al.*, Appl. Phys. Lett. **74**, 3281 (1999).
[25] L. Shi, F. A. Ponce, and J. Menendez, Appl. Phys. Lett. **34**, 3471 (2004).
[26] C. Bungaro, K. Rapcewicz, and J. Bernholc, Phys. Rev. B **61**, 6720 (2000).
[27] J. C. Nipko, C. K. Loong, C. M. Balkas, and R. F. Davis, Appl. Phys. Lett. **73**, 34 (1998).
[28] H. Harima, H. Sakashita, T. Inoue, and S. Nakashima, J. Cryst. Growth **189/190**, 672 (1998).
[29] H. Harima, T. Inoue, S. Nakashima, K. Furukawa, and M. Taneya, Appl. Phys. Lett. **73**, 2000 (1998).